Robinia pseudoacacia, a nitrogen-fixing tree, facilitates the current and future growth of neighboring trees

Alexa Helms

Submitted in partial fulfillment of the

Requirements for the degree of

Master of Arts

in Ecology, Evolution, and Conservation Biology

Department of Ecology, Evolution, and Environmental Biology

COLUMBIA UNIVERSITY

May 19th, 2020

Abstract

Trees that can form symbioses with nitrogen (N)-fixing bacteria (N-fixers) have long been thought to facilitate neighbors by providing new N to the ecosystem. However, empirical assessments have shown that N-fixers can have the full range of impacts on neighboring trees: facilitation, no effect, or inhibition. Two possible explanations for the wide variation in N-fixers' impacts on their neighbors are that (1) facilitation via increased N supply might have a substantial time lag, whereas most studies have examined a single census interval, and (2) N-fixers may down-regulate the amount of N they fix as succession proceeds. In this study, we examined how N-fixing *Robinia pseudoacacia* L. trees impacted the growth of neighboring trees throughout their lifespan using tree cores to estimate growth rate. We also measured the natural abundance of $\delta^{15}N$ values of tree cores, which we used to estimate the percent of a tree's N it derived from fixation ($\%N_{dfa}$). In the one site where we could meaningfully constrain $\%N_{dfa}$, our mean estimate was that *Robinia* fixed greater than 51% of its N throughout its 60-year lifespan, though there was substantial uncertainty in each estimate. From the tree core ring widths, we found that *Robinia* facilitated the growth of neighboring non-fixing trees, but inhibited the growth of neighboring N-fixing trees. Importantly, we found evidence that *Robinia*'s facilitation effect grew stronger with lag times, peaking at 14 years, indicating that it enhanced the future growth of neighboring trees. Our observation of this lag effect matches with biogeochemical expectations, and indicates that single-census studies might underestimate the degree to which N-fixers facilitate forest growth.

Introduction

Symbioses between plants (known as N-fixers) and bacteria that fix N_2 into plant-available NH_3 can bring in over 100 kg N ha^{-1} yr^{-1} into a forest environment (Binkley et al. 1994; Ruess et al. 2009), and thus can stimulate rapid plant growth (Batterman et al. 2013). Although largely unaddressed in the literature, it is also likely that this impact on forest growth becomes more profound over time. This is especially true as N-fixation rates, which have often been impractical to measure, potentially change throughout an individual tree's lifespan. These unknowns continue to cloud our understanding of N-fixers' effect on forest growth.

Fertilization and competition are two possible mechanisms by which N-fixers may influence forest growth. On average, N-fixers have a higher foliar N content than non-fixing trees (Adams et al. 2016; Nasto et al. 2014; Fyllas et al. 2009; Townsend et al. 2007), as well as a higher rate of leaf decay (Wedderburn and Carter 1999). This allows leaf litter from N-fixers to more quickly return fixed N to the soil, enriching the available soil N pool and thus increasing forest growth. Neighboring trees may also access fixed N through root exudates or interconnected mycorrhizal networks (Hoogmoed et al. 2014). Fertilization, however, is not an immediate process and likely occurs on a time delay. First, fixed N must move from the roots of a N-fixer to its leaves. The leaves must then fall and decay before the N can traverse the soil to a neighboring tree's roots. Possibly, some litter will clump near the base of the N-fixer, hindering how quickly it can then spread to neighboring trees. It is unclear how long, or how consistently, this process happens. It is clear, however, that growth facilitation from fertilization can only occur within a time lag.

Despite fertilization, N-fixers can inhibit forest growth by being better competitors than neighboring trees. N-fixers are typically early successional species and thus tend to have higher growth rates than non-fixing trees (Batterman et al. 2013; Menge and Chazdon 2016). This

allows N-fixers to become canopy dominant earlier, out-competing neighboring trees for light-availability (Taylor et al. 2017). Additionally, N-fixers may be better competitors for nutrients. The high N content of N-fixers may allow them to have increased photosynthetic rates, a higher water use efficiency (Adams et al. 2016), and better access to soil phosphorus (Houlton et al. 2008; Perakis and Pett-Ridge 2019). Competition, much like with fertilization, must occur on a time delay. Most likely the inhibitory effect from a canopy-dominant N-fixer would be greatest after several years had passed and the neighboring trees had been sufficiently starved of resources. By considering the effects of fertilization and competition, especially how they interact through time, we are able to understand how N-fixers may impact forest growth.

Although the relationship between N-fixers and forest growth remains uncertain, much work has been done to expand our understanding of the topic. Many studies have found evidence that N-fixers promote forest growth. For example, N-fixing red alders (*Alnus rubra* Bong.) increased both the forest biomass and net primary productivity of 55 year-old Douglas-fir (*Pseudotsuga menziesii* (Mirbel) Franco) stands in southwestern Washington (Binkley et al. 1992). Similarly, *Eucalyptus* trees also had increased productivity when planted in mixed stands with N-fixers (Forrester et al. 2006). Here the increases in primary productivity and forest biomass equate to a facilitation of forest growth due to the presence of N-fixers. Two chronosequence studies, which were able to consider the impact of N-fixers through time, found that N-fixers increased total stand N over 300 years in Panama (Batterman et al. 2013) and over 37 years in south Appalachian forests (Boring and Swank 1994). While an increase in total stand N may not immediately indicate facilitation, it allows for higher availability of a potentially limiting nutrient, which, in turn, likely promotes growth. Most recently, a study was conducted using the FIA database to compare the impacts of N-fixing trees, largely *Robinia pseudoacacia*

L., across 3837 ha of forest throughout the United States. N-fixers tended to facilitate overall basal area and non-fixing tree biomass, but with a high degree of variation between plots (Staccone et al. in review). Although these studies indicate that N-fixers facilitate forest growth, recent experiments have demonstrated that this is not always the case. A 5-year study in Panama found N-fixers had no impact on the growth of neighboring trees (Lai et al. 2018). Additionally, a long-term experiment in the Alaskan floodplain found that N-fixing thinleaf alder (*Alnus incana* (L.) Moench), after an initial facilitation, inhibited survivorship and growth of neighboring white spruce (*Picea glauca* (Monench) Voss) (Chapin et al. 2016). Similarly, the growth of a Costa Rican forest was inhibited by the presence of a variety of N-fixers (Taylor et al. 2017). These studies demonstrate that the impact N-fixers may have on forest growth can be highly variable. It is also clear that our current understanding of N-fixers lacks a temporal element. With few exceptions (Chapin et al. 2016), our current view of how N-fixers interact with neighboring trees relies on studies with static temporal forest dynamics.

While all of the previous studies have enhanced our understanding of the influence of N-fixers on forest growth, they were unable to consider the past influences of N-fixers on forest dynamics. As previously stated, it is likely that any effect from N-fixers occurs with a time lag. The difference between past and present dynamics could prove to be crucial to our understanding of forest interactions. One of the only long-term studies on this topic, Chapin et al. (2016), made that apparent. For the first several years of the experiment, N-fixing *Alnus incana* facilitated the growth of the forest stand. Afterwards, the N-fixers had a prominent inhibition effect, demonstrating how crucial the often missing temporal component is to our understanding of forest dynamics. Unfortunately, it is often impractical to conduct long-term experiments, as they are frequently costly and slow. Chronosequences have been favored as a way to study both the

117 impacts of N-fixing trees and the rates at which N-fixation happens. However, because
118 chronosequences necessarily study different sites, site-specific factors cloud the cross-age
119 comparisons (Chazdon et al. 2007; Feldpausch et al. 2007). This inherent issue with
120 chronosequences, combined with the challenges of measuring N-fixation itself (Shearer and Kohl
121 1986; Unkovich and Pate 2000; Winbourne et al. 2018), means that the estimates of fixation
122 rates and the impacts of N-fixers are relatively uncertain.
123 N-fixation rates have historically proven tricky to measure. Many methods to determine
124 N-fixation rates have been developed based upon isotopic N values, as N-fixation measurements
125 can be based on the abundance of stable N isotopes (^{15}N versus ^{14}N) in N-fixing plants (Shearer
126 and Kohl 1986). Unfortunately, these studies typically require isotopic enrichment (financially
127 exhaustive) followed by foliar ^{15}N measurements, which provide fixation rates for only one point
128 in time. However, the information left behind in annual tree rings offers an appealing way to
129 overcome some of the challenges in studying N-fixation through time. The widths of annual tree
130 rings yield insight into past growth rates (Stokes 1996; Beghin et al. 2011) and likely the N in the
131 tree rings gives information about past fixation. The natural abundance method compares the
132 isotopic signals of a focal N-fixing plant to a neighboring non-fixing ("reference") plant and to
133 the signal of pure N-fixation (Shearer and Kohl 1986). The underlying assumption is that the
134 reference plant samples the same soil N pool in the same way as the N-fixer. When the isotopic
135 signal of the reference plant is sufficiently distinct from the pure fixation signal, it is possible to
136 estimate N-fixation. There are a number of issues with the isotopic method, particularly when
137 used for sub-annual timespans (Soper et al. 2015), but no method of measuring fixation is perfect
138 (e.g., Shearer and Kohl 1986; Unkovich and Pate 2000; Winbourne et al. 2018). When this
139 method is used on foliage, it captures the fixation activity for each growing season (for

deciduous trees). With tree cores, however, it might be possible to capture N fixation through decades of ontogenetic development of trees. Several studies have pioneered methods of measuring nitrogen isotope ratios in tree cores (Saurer et al. 2004; Hietz et al. 2011). Because N can be recovered from dying cells and re-translocated to form new tissues during the process of converting from sapwood to heartwood (Merrill and Cowling 1966; Meerts 2002), this method is not ideal for pinpointing exact years, but over spans of multiple years it gives useful information (McLauchlan et al. 2010). To our knowledge, no studies have used tree core nitrogen isotopes to infer N-fixation rates. Using tree cores to measure N-fixation rates addresses gaps the literature was previously unable to consider: how often N-fixing trees are actually fixing, how those rates change through time, and from that how N-fixers are influencing neighboring trees through time.

Robinia pseudoacacia L. is the dominant N-fixer in temperate forests of the Northeastern United States (Menge et al. 2010; Liao and Menge 2016; Staccone et al. 2020). Decades ago, Boring and Swank (1984) measured N-fixation rates of *Robinia* along a 64-year chronosequence, finding a higher fixation flux at 17 years old than at 4 or 38 years old. This shows that *Robinia* possibly changes its fixation rates throughout its lifespan, and thus may impact the growth of the forest differently as it ages. Since then, there have been a number of advances in the understanding of *Robinia*. For instance, it is quite resistant to drought (Minucci 2017), even increasing its fixation rate in drier conditions (Wurzburger and Miniat 2014). We also know more about its abundance and demographics through succession: across the United States, its growth and recruitment rates decline substantially during the first 50 years of succession, and its mortality rates remain relatively high (Liao and Menge 2016). However, our understanding of how *Robinia* changes its fixation rates through succession have not advanced. Additionally, while it seems that *Robinia* may facilitate the growth of neighboring trees (Boring and Swank 1984;

Schuster and Hutnik 1987; Staccone et al. in review), it is still unknown how *Robinia* affect forest growth through time. In this study, we used the widths of annual tree rings for both *Robinia* and neighbors to calculate annual growth rates, the neighborhood crowding index, and isotopic N signatures. This allowed us to provide clarity on a previously unused method to measure N-fixation through a N isotope presence in tree cores and determine how *Robinia* fixation rates may change through time. This study also allowed us to understand how N-fixing *Robinia* impacts current and future forest growth. Specifically, we have determined 1) how N-fixation by *Robinia* changes throughout its lifespan and 2) whether the growth rates of neighboring trees are facilitated or inhibited by past and current crowding from N-fixing *Robinia*.

Methods

Field Site

Our work took place in Black Rock Forest (41°24' N, 74°01' W), a 1550-ha forest preserve dominated by oak (*Quercus* spp.) (Figure 1) (Schuster et al. 2008). The mean annual precipitation is 1.2 m and the mean monthly temperature ranges from -2.7 °C to 23.4 °C from January to July (Schuster et al. 2008). We collected data from two sites, the Stone House (SH) site (41°24'0" N, 74°01'0" W) and the Upper Reservoir (UR) site (41°25'0" N, 74°0'0" W). The SH site contained 12 *Robinia* and 21 non-fixing trees consisting of *Acer saccharum* Marshall (1), *Fraxinus americana* L. (1), *Juglans nigra* L. (1), *Liriodendron tulipifera* L. (1), *Picea abies* (L.) H. Karst. (2), *Picea glauca* (Moench) Voss (12), and *Prunus serotina* Ehrh. (3). This site had been clear cut in the 1930s and was planted with *P. glauca* in the 1940s (Bill Schuster, personal communication 2019). The *Robinia* present likely grew in naturally. The UR site contained 37 *Robinia* and 46 non-fixing trees consisting of *Acer rubrum* L. (16), *Betula lenta* L. (1), *F. americana* (17), *P. serotina* (2), *Salix nigra* Marshall (1), and *Quercus rubra* L. (3). This site was

187 burned in 1911 and by the 1930s was a pasture and farm (Bill Schuster, personal communication
188 2019). *Quercus, Fraxinus, Prunus,* and *Acer* were later planted on the site; *Robinia* likely grew
189 naturally. The UR site is located near a stream and a reservoir, with various depressions. It is
190 located at a lower elevation (between 286 and 280 m above sea level) than the SH site (between
191 390 and 384 m).
192
193 *Sample Collection*
194 At each site we mapped trees that were > 10 cm diameter at 1.3 m height (DBH).
195 Specifically, we mapped all *Robinia* trees, all trees within 10 m of a *Robinia* tree (*Robinia*
196 neighbors), and all trees within 10 m of a *Robinia* neighbor. We measured tree diameter with
197 DBH tape. We mapped the location of trees by measuring the distance and angle from a set point
198 to the center of each tree. At least one core was taken at 1.3 m height from any tree that was not
199 visibly rotten. Tree ring widths from cores were used to calculate growth rate data and to
200 estimate annual tree diameter through each individual tree's lifespan.
201 Additionally, we took two cores (perpendicular to each other) from 5 *Robinia* and 5
202 neighboring *Prunus* trees for $\delta^{15}N$ isotopic analysis (3 *Robinia* and 3 *Prunus* from SH and 2
203 *Robinia* and 2 *Prunus* from UR). *Prunus* trees were explicitly chosen as reference trees due to
204 their arbuscular mycorrhizal association (the same as *Robinia*) and their presence on both field
205 sites.
206 All data were collected between December 2018 and August 2019.
207
208 *Measurement of Ring Widths and Growth Rates*
209 Tree cores were fully dried before being glued on to wooden mounts with the vessels
210 facing upwards. Once dry, the cores were sanded with increasingly fine graded sandpaper until

yearly rings were clearly visible and distinct under a sliding microscope. Years were assigned to rings starting from the outermost ring and moving inward to the pith. Annual ring widths were measured using a sliding microscope and the iMeasure computer program and confirmed using the computer program COFECHA (a quality test to confirm that the cores were measured properly) (ITRDB Program Library; Holmes 1997). Annual ring widths were then used to calculate the relative diameter growth rates of each individual tree, calculated as

$$gr_{t,i} = \frac{\ln(d_{t+\Delta t,i}) - \ln(d_{t,i})}{\Delta t} \quad \text{Eq.1}$$

where $d_{t+\Delta t}$ was twice the total core length for t to time t + Δt and i was any individual tree. In this case, Δt was always 1 year. In cases where multiple cores were taken, the mean annual ring widths in each year were used to calculate relative growth rate. The number of rings present were used to determine the minimum age of the trees at coring height, as it is not always possible to core to the pith of a tree.

Neighborhood Crowding Index

Neighborhood Crowding Index (NCI) is a metric used to quantify the degree of crowding experienced by a focal tree. Crowding increases with the number of neighbors within (here, 10 m; based on Canham et al. 2004), their size, and their proximity to the focal tree. Specifically, NCI was calculated as

$$NCI_i = \sum \frac{DBH_j^2}{d_{j,i}^2} \quad \text{Eq. 2}$$

where NCI of an individual tree *i* is the sum of the squared DBH of all neighbors *j* divided by the squared distance of all neighbors *j* to focal tree *i* (Canham et al. 2004). Further, to consider the effect of crowding from N-fixers, as opposed to non-fixers, we calculated the proportion of NCI containing N-fixers, following Taylor et al. (2017) and Staccone et al. (in review 2020):

$$NCI_{prop,i} = \frac{NCI_{N-fixer}}{NCI_{total}} \quad \text{Eq. 3}$$

Here both NCI and NCI_{prop} were calculated from tree ring data where DBH is twice the core length for t to time t + Δt. Thus, we have calculated past NCI throughout each tree's life span, excluding any trees that may have perished prior to the sampling year.

Pre-Processing of Tree Cores and Measurement of N Isotopes

Cores from the selected *Robinia* ("focal") and *Prunus* ("reference") trees were pre-processed for $\delta^{15}N$ isotopic analysis by modifying methods described in Sheppard and Thompson (2000). Cores were analyzed in 5-year segments because finer resolution could be confounded by N leaching across rings after growth and to meet the minimum sample size requirement for analysis (Gerhart and McLauchlan 2014). Segments were then submerged in a 1:1 toluene and ethanol mixture for two nights, with the mixture replaced after the first 24 hours. The mixture was decanted and the cores were submerged in ethanol overnight. Then, the cores were submerged in deionized water overnight. This process removed any labile N compounds, secondary plant compounds, inorganic salts, and small polysaccharides. Lastly, the cores were dried at 60 ºC and ground into a fine powder using a ball grinder (GlenMills, Clifton, NJ). Any segments from the same individual from the same time segment were ground and sampled together. Samples were then packed in tin capsules and shipped to UC-Davis Stable Isotope lab. There the samples were analyzed for $\delta^{15}N$ values using a PDZ Europa 20-20 isotope ratio mass spectrometer (Sercon Ltd., Cheshire, UK). $\delta^{15}N$ is calculated based on $^{15}N/^{14}N$ isotopic ratios, where

$$\delta^{15}N = \left(\frac{\frac{^{15}N}{^{14}N}_{sample}}{\frac{^{15}N}{^{14}N}_{atmospheric\ N_2}} - 1 \right) 1000 \quad \text{Eq. 4}$$

Estimate of Percent Nitrogen derived from Fixation

The percent of nitrogen derived from fixation (% N_{dfa}) can be determined from natural ^{15}N abundances by comparing the isotopic signature of N atoms in N-fixing plant biomass to that of non-fixing plant biomass when soil N is sufficiently more ^{15}N-enriched than atmospheric N (Shearer and Kohl 1986). Specifically, % N_{dfa} is calculated using an equation based on Shearer and Kohl (1986):

$$\%N_{dfa} = \left(\frac{\delta_f - \delta_r}{\delta_b - \delta_r}\right) 100 \quad \text{Eq. 5}$$

Here δ_f is the $\delta^{15}N$ value from the N-fixing tree (*Robinia*), δ_r is the $\delta^{15}N$ value of the non-fixing reference tree (*Prunus*), and δ_b is the isotopic signature of foliar N from pure N-fixation. Here, we used -1.2‰ for δ_b (Mantovani et al. 2015) with a standard deviation of 0.5‰ as literature reports a range of -2‰ to 1‰, where the most common values is near -1‰ (Kohl and Shearer 1980; Doughton et al. 1992; Boddey et al. 2000).

The reference trees are critical for the success of this method since many of the assumptions of the $\delta^{15}N$ method depend on a suitable reference. Ideally, reference trees should sample from the same soil N pool as the N-fixer and exhibit similar within-tissue fractionation (Shearer and Kohl 1986). Because our study focuses on tree rings, the reference trees should also have been present throughout the same time span as the N-fixer. Thus, we chose the reference trees that were close to the focal tree (within 10 m) while present during the same timespan (based on tree ring data; *Prunus* were 49 - 64 years old and *Robinia* were 49 - 69 years old), and had the same mycorrhizal association as the focal *Robinia* trees. For this reason, it is likely that reference trees were sampling soil N from the same pool at the same time and in a similar manner to the focal N-fixers.

We bootstrapped $\%N_{dfa}$ values 10,000 times for each tree at each 5-year time segment to calculate confidence intervals of each $\%N_{dfa}$ value (Taylor and Menge 2018). The means and 95% confidence intervals from the bootstrapped distributions were used to display the $\%N_{dfa}$ estimates. We assumed normal distributions of δ_f, δ_r, and δ_b. The means and standard deviations of δ_r for the SH site were calculated based on the arithmetic mean and standard deviations of all reference trees present on the site. The means and standard deviations of δ_r for the UR site were specific to the individual reference trees, as they were more than 10 m apart from each other and were paired with specific N-fixers.

Data Analysis

Our data analysis is tailored to our two questions. First, to address how N fixation by *Robinia* changed through tree age, we followed the likelihood approach in Menge et al. (2015), which models how $\%N_{dfa}$ changes along a gradient and incorporates uncertainty in the distribution of the end members of an isotopic mixing model (Phillips and Gregg 2001). Specifically, we compared two models of how $\%N_{dfa}$ might change with tree age: A linear change with tree age and no change with tree age.

We minimized the negative log likelihood of the $\delta^{15}N$ data for each model, including variation in both the end member $\delta^{15}N$ and the sample $\delta^{15}N$ as follows:

$$NLL = -\sum_i \ln\left(Normal(\delta^{15}N_{sample,i} | \delta^{15}N_{expected,i}, \delta^{15}N_{sd,i})\right) \quad \text{Eq. 6}$$

$$\delta^{15}N_{expected,i} = \left(\frac{\%N_{dfa\ expected,i}}{100}\right)\delta^{15}N_{fixation,mean} + \left(1 - \frac{\%N_{dfa\ expected,i}}{100}\right)\delta^{15}N_{reference\ mean,i} \quad \text{Eq. 7}$$

$$\delta^{15}N_{sd,i} =$$

$$\sqrt{\left(\left(\frac{\%N_{dfa\ expected,i}}{100}\right)\delta^{15}N_{fixation\ sd}\right)^2 + \left(1 - \left(\frac{\%N_{dfa\ expected,i}}{100}\right)\delta^{15}N_{reference\ sd,i}\right)^2 + \delta^{15}N_{sample\ sd,i}}$$

Eq.8

For these models, we considered the SH and UR sites separately.

Second, to address how crowding by *Robinia* influenced the growth of its neighbors, we controlled for factors known to influence growth, then isolated the proportion of crowding by *Robinia* as our target driver variable.

Specifically, we modeled relative growth rate (log-transformed to ensure normality) as a function of the total NCI around an individual, the DBH of the individual, and the proportion of NCI from *Robinia* (SI Text 1). We considered a variety of different versions, including and excluding interaction terms and quadratic terms. We also ran a version of the model considering N-fixers and non-fixers separately, as a binary term (SI Text 1). To address the possibility of lag effects between the presence of *Robinia* and neighbor growth rate, we also considered the relationship between relative growth rate and past crowding from 1-20 years ago (SI Text 1).

We determined the best model, with the exception of models containing a time lag, based on the lowest AIC values, and also presented any other model within 2 delta AIC units. For lagged models, we used the structure of the best fit model from the non-lagged model, but with the proportion of NCI from fixers from past years. We also ran lagged models with the proportion of NCI from fixers from past years and the total NCI from past years. Lagged models contained fewer datapoints than the current models because not all trees are the same age. All analyses were implemented in R (R Core Team 2018).

Results

322 *$\delta^{15}N$ and $\%N_{dfa}$*

323 For both the SH and UR site, the best fit model allowed for variation within N-fixer
324 intercept values, but not for slope (Eq. 6-8). There was significant site variation for the $\delta^{15}N$
325 values of the reference trees, which impacted how precisely we could calculate $\%N_{dfa}$. At the UR
326 site, the mean reference $\delta^{15}N$ value was 0.26‰, which led to unconstrained $\%N_{dfa}$ values as it
327 was not far enough away from the value of pure fixation for the degree of variation in each end
328 member. By "unconstrained," we mean that the confidence limits on the % of a plant's N derived
329 from fixation extended both below 0% and above 100%, which is not informative. Yet, the
330 modeled values for each individual *Robinia* were 32% and 54%, with an average of 43 $\%N_{dfa}$
331 and a mean $\delta^{15}N$ of -0.46‰ (SI Table 1, Figure 1a, c). For these calculations, *Robinia* did not
332 decrease the rate of fixation throughout its lifespan. At the SH site, the mean reference $\delta^{15}N$
333 value was 2.82‰. This value is far enough from the pure fixation value, compared to the
334 variation in each end member, to provide a constrained $\%N_{dfa}$ estimate, although the uncertainty
335 of each estimate is still wide. The individual modeled mean values for each tree were 55%, 54%,
336 and 45%N_{dfa} (SI Table 1, Figure 1b, d). Therefore, on average, at the SH site *Robinia* fixes 51%
337 of its N throughout its life, where the mean $\delta^{15}N$ value was 1.147‰. At this site, *Robinia* fix less
338 N as they age at a rate of 0.2% less per year. That means that, on average, a tree derives 50% of
339 its N from fixation when it is 5 years old, but 41% when it is 50 years old. While this is
340 statistically significant, the decrease is incredibly slight and likely biologically meaningless
341 given the inherent uncertainty of this method.

342 *Growth Rate*

343 The growth rate model with the lowest AIC ($R^2 = 0.4986$, SI Table 2, Figure 2) had linear
344 terms for NCI, DBH, and NCI_{prop}, along with an interaction between DBH and NCI:

$$\ln(RGR_i) = \alpha + \beta_1 \times NCI_{prop,\,j} + \beta_2 \times DBH_i + \beta_3 \times NCI_i + \beta_4 \times DBH_i \times NCI_i + \varepsilon \quad \text{Eq. 9}$$

For all models, α is the overall intercept, βs are the regression coefficients, and ε is the normally distributed error term. All of the best models were linear with the driver variable of interest, the proportion of NCI from *Robinia.* The next best model, 1.13 delta AIC units worse than the former ($R^2 = 0.4985$, SI Table 3, SI Figure 1a), included a quadratic term for crowding:

$$\ln(RGR_i) = \alpha + \beta_1 \times NCI_{prop,\,i} + \beta_2 \times DBH_i + \beta_3 \times NCI_i + \beta_4 \times NCI_i^2 + \beta_5 \times DBH_i \times NCI_i + \varepsilon \quad \text{Eq. 10}$$

Overall, the current (unlagged) proportion of crowding from N-fixers significantly increased the growth rate of neighboring trees. Specifically, growth rate would increase by approximately 18% when going from no crowding from N-fixers to only crowding from N-fixers (Table 1). Unsurprisingly, both models found that growth decreased as total crowding tree size increased (SI Tables 2-3).

The growth rate model which considered N-fixers and non-fixers separately with the lowest AIC had a single interaction (between the control drivers, DBH and NCI) and no quadratic term:

$$\ln(RGR_i) = \alpha + \beta_1 \times NCI_{prop,\,i} + \beta_2 \times DBH_i + \beta_3 \times NCI_i + \beta_4 \times \text{N-fixer} + \beta_5 \times \text{N-fixer} \times NCI_{prop,\,i} + \beta_6 \times DBH_i \times NCI_i + \varepsilon \quad \text{Eq. 11}$$

The next best model, 0.61 delta AIC units worse than the former, included a quadratic term for crowding:

$$\ln(RGR_i) = \alpha + \beta_1 \times NCI_{prop,\,i} + \beta_2 \times DBH_i + \beta_3 \times NCI_i + \beta_4 \times NCI_i^2 + \beta_5 \times \text{N-fixer} + \beta_6 \times \text{N-fixer} \times NCI_{prop,\,i} + \beta_7 \times DBH_i \times NCI_i + \varepsilon \quad \text{Eq. 12}$$

Similar to the models above, we found that the proportion of crowding from N-fixers significantly increased the growth rate of neighboring, non-fixing trees. However, this model found that as the proportion of crowding from N-fixers increases, the growth rate of neighboring N-fixers decreased (best model: $R^2 = 0.502$, SI Table 4, Figure 2; next best model: $R^2 = 0.502$, SI Table 5, SI Figure 1b). Specifically for the best fit model, the expected growth rate of a non-fixer would increase by 14% when surrounded by N-fixers compared to non-fixers. In contrast, the expected growth rate of an N-fixer would decrease by 5% when surrounded by N-fixers compared to non-fixers (Table 1). The results were similar for the next best fit (Table 1). As above, both models found that growth decreased as total crowding tree size increased and that the quadratic term, NCI^2 had no significant impact on growth rate.

The best lagged models contained NCI_{prop} from 1 through 20 years prior to current growth rates as follows:

$$\ln(RGR_i) = \alpha + \beta_1 \times NCI_{prop,\, i,\, lagged\ year} + \beta_2 \times DBH_i + \beta_3 \times NCI_i + \beta_4 \times DBH_i \times NCI_i + \varepsilon \quad \text{Eq. 13}$$

Past crowding from N-fixers increased the current growth of non-fixing neighboring trees more so than current crowding from N-fixers ($R^2 = 0.4812$, SI Table 6). Here, growth rate increased by nearly 15% when going from no crowding from N-fixers one year ago to only crowding from N-fixers one year ago (Table 1). Additionally, we found that the effect of past crowding increased and peaked at crowding from 14 years in the past (Figure 3). In lagged models containing both past NCI_{prop} and past NCI_{total}, the best model containing the highest adjusted R^2 value was also lagged one year. This model output also found that the impact of N-fixer crowding increased with time passed and peaked at 14 years (SI Figure 2).

Discussion

Robinia increased N inputs to these forests by fixing an estimated 43% or more of their N throughout their lifetime. Assisted by this mechanism, *Robinia* are actively facilitating the current and future growth of neighboring non-fixing trees. They also inhibit the current growth of neighboring N-fixing trees.

Our findings on $\%N_{dfa}$ for *Robinia* are consistent, although slightly lower, with the current literature. Typically, it has been shown that *Robinia* can fix anywhere between 58% - 94% of its N (Mantovani et al. 2015; Danso et al. 1995; Marron et al. 2018). Previous studies were conducted by measuring $\delta^{15}N$ of the leaf, branches, stems, and/or roots of the tree at one specific timepoint. Our study measured $\delta^{15}N$ of tree cores, estimating *Robinia* to fix 51% for the SH site and 43% for the UR site (Figure 1c, d). It has been shown that the most accurate calculations of $\%N_{dfa}$ occur when all parts of the tree are sampled, as sampling only one section tends to result in a slightly higher or lower estimate depending on which part of the tree is sampled (Danso et al. 1995). Thus, it is possible that lower values we observed occurred as we sampled only from one section of the tree. Further, the data from the UR site had wide confidence intervals and are likely a poor estimate, unlike that of the SH site. Site variation is a common issue when measuring N-fixers and is often linked to environmental factors. The UR site, located between a stream and a reservoir, is more likely to have higher soil moisture, an abiotic factor known to affect N-fixers. Chapin et al. (2016) found higher mortality of N-fixers as well as less direct and more variable inhibitory effects from N-fixers on sites with greater soil moisture. High soil moisture has also been linked to greater facilitation of BAI and recruitment from N-fixers (Staccone et al. in review) as well as lower competition from N-fixers (Gei et al. 2018; Liao and Menge 2016, Minucci 2017; Pellegrini et al. 2016; Wurzburger and Miniat 2014). While species differences likely played a role in variation between N-fixer responses, it is

clear that soil moisture is key to the success of N-fixers. Here, soil moisture or other unmeasured abiotic factors possibly played a role in how accurately we were able to calculate $\%N_{dfa}$ at the UR site. While the total amount of N derived from fixation assists in our understanding of the process, it is perhaps more critical to learn how fixation changes over time.

We also found that *Robinia* very slightly its decreased fixation rate throughout its lifespan (Figure 1c). This is consistent with the idea that the amount of ecosystem N-fixation increases and then decreases from early to late succession (Boring and Swank 1984; Viereck et al. 1993; Pearson and Vitousek 2002; Uliassi and Ruess 2002; Menge and Hedin 2009; Batterman et al. 2013; Sullivan et al. 2004). This occurs as available soil N pool increases potentially causing N-fixers to downregulate fixation. The total number of N-fixers may have also thinned due to increased competition as the forest ages. There is currently no evidence on the fixation strategy of *Robinia*, nor do we have any information on the fluxes between or the abundance of the soil N pool at either of our sites. Thus, we cannot say for certain if *Robinia* is downregulating in response to higher soil N availability. However, it was found that in North Carolina, *Robinia* had higher N fixation fluxes (75 kg N ha^{-1} y^{-1}) in 17-year-old stands compared to 38-year-old stands (33 kg N ha^{-1} y^{-1}) (Boring and Swank 1984), which indicates that *Robinia* is capable of downregulation. It should also be noted that while statistically, there appeared to be a decrease in fixation rates, estimates for $\%N_{dfa}$ using the natural abundance method may not be able to accurately show changes of 0.2% (Figure 1c). Additionally, such a slow rate of decrease may not be biologically significant. In this case, *Robinia,* on average fix 51% of their N at age 1, meaning they would still fix 31% after 100 years, longer than most *Robinia* live. As *Robinia* have shown to fix fairly large amounts of N throughout their lifespan, it is likely they are enriching the available soil pool for nearby trees.

We found that the presence of N-fixers facilitates the contemporary growth of neighboring trees (Figures 2-3), which is consistent with the majority of research on the topic (Siddique et al. 2008; Staccone et al. in review 2020; Hoogmoed et al. 2014; Forrester et al. 2006; van Kessel et al. 1994). While fertilization is likely the main mechanism for facilitation, N-fixers may also facilitate neighbors by being worse competitors than non-fixing neighbors (Taylor et al. 2017; Staccone et al. in review). Although most N-fixers do have higher growth rates than non-fixing trees, *Robinia* has lower growth rates and higher mortality rates than non-fixers in the United States (Liao and Menge 2016). Additionally, there has been evidence that N-fixers may not be good competitors for soil P (Soper et al. 2015; Nasto et al. 2014; Batterman et al. 2013). Thus, *Robinia* may facilitate the growth of non-fixers both through fertilization and by being weak competitors. We also found that N-fixers, while facilitating the growth of non-fixing neighbors, inhibit the growth of N-fixing neighbors (Figure 3). A study in Costa Rica also found that N-fixers inhibit other N-fixers roughly 15% more than they inhibit non-fixers (Taylor et al. 2017). As those N-fixers were located in a tropical area, where N availability is high, the inhibition of N-fixer growth likely occurred due to a combination of 1) the high nutrient demand of N-fixers and 2) non-fixers not being limited by N. While our study occurs in a temperate forest, where N availability is typically low, we know that N-fixers are fixing N and that the fixed N is very likely being absorbed by non-fixing neighbors, resulting in the facilitation of growth. For this reason, non-fixing neighbors on our sites may also not currently be limited by N. Thus the inhibition of N-fixer growth we observe may be due to the high cost of N-fixation itself. The required allocation of C to nodules to support N-fixation can result in lower growth, an effect which has been observed globally in both trees and crops (Minchin and Witty 2005; Schulze et al. 1999; Shi et al. 2016).

Additionally, we have found that the presence of N-fixers facilitates the future growth of neighboring trees to an even greater degree than it does current growth, a dynamic which has not been previously considered in the literature. Facilitation of future growth is likely due to a time delay between when *Robinia* are fixing N and when that N is made available to neighboring trees. Our research indicates, however, that the highest impact on neighboring tree growth occurs when N-fixers have been present for 14 years (Figure 5). This further confirms that *Robinia* are in fact fertilizing the soil, resulting in a build-up of soil N. Batterman et al. (2013) found that within the first 25 years, N-fixers exceeded the forest demand for N, before a resulting N deficit trend. In our study, the impact N-fixers have on forest growth begins to decrease after 14 years. Further, it is important to note the distinction between our study and previous research. Previous studies were limited to examining how N-fixers and their neighbors interacted in the past. Here, we were able to observe how past N-fixers impact current neighbors. This distinction is critical to understanding not only the effect N-fixers may have on forest growth, but the legacy effects they may have on future growth.

Only one study thus far has considered the potential legacy effects of *Robinia.* Schuster and Hutnik (1987) found that the basal area of invading tree species, specifically *Prunus*, were highest on plots containing *Robinia* trees. Further, they noted that there was an overall decline in *Robinia* populations. Combined, this paper hints at the prospect that as *Robinia* die, they fertilize the soil and facilitate the growth of any new-coming trees, allowing succession to continue. Here, in addition to fertilization from N-fixation, it is likely that the decay of deceased *Robinia* trunks are resulting in large inputs of N into the available soil pool, with an undetermined time delay, facilitating the growth of trees. Our study indicates that the relationship between N-fixers and neighboring trees may be more complex than that. While it is likely that *Robinia* input great

amounts of N into the soil once they decay, the active presence of *Robinia* aiding in a continuous build-up of N likely also plays an important role in forest growth.

Although N-fixation rates are the focus of this study, important information can be derived from the isotopic ratios of non-fixing trees. How $\delta^{15}N$ values of non-fixing trees change with age have been used to document fluctuations within the local (Saurer et al. 2004) and global (Hietz et al. 2011) nitrogen cycles, spanning from the 1920s-1960s. Here, our non-fixing trees did not appear to show any discernable trends throughout their 50 – 60 year lifespans (Figure 1a, b).

In general, using the natural abundance of nitrogen isotopes to estimate $\%N_{dfa}$ has well-known caveats (Shearer and Kohl 1986; Soper et al. 2015). Our propagation of variation in soil N and pure fixation end-members provides more accurate estimations, but does not overcome the limitations of the method entirely. As demonstrated by the UR site results, a soil N signal too close to the pure fixation signal renders uninformative estimates (Figure 1c). Unconstrained soil N signals can occur for a wide variety of reasons. Possibly, the non-fixing reference trees were being more actively fertilized by the N-fixers than on the SH site, and thus had $\delta^{15}N$ values more similar to that of the N-fixing trees. The references trees may also have accessed different soil pools from those of the N-fixing trees. Further, the N-fixing trees themselves may have recycled their fixed N through resorption or by re-consuming fixed N. N fixation rates, however, are notoriously difficult to measure with any method (Shearer and Kohl 1986; Unkovich and Pate 2000; Soper et al. 2015; Winbourne et al. 2018). Nodules are often hard to sample and have patchy distributions; nodule activity varies spatially and temporally; enriched isotopes both have similar issues to natural abundance isotopes and are financially exhaustive. There are, however, distinct advantages of using the natural abundance isotope method on tree cores. Specifically, we

are able to track $\%N_{dfa}$ through individual trees without making assumptions about site differences, as is required with chronosequences. This allows us to more confidently estimate how individual trees adjust their fixation rates through time. Therefore, it is our hope that this tree-core $\delta^{15}N$ method will be an additional tool in ecosystem ecologists' toolbox.

In conclusion, all of our findings were consistent with the current research and addressed gaps in the literature not previously considered. To our knowledge, this study was the first to quantify N-fixation rates by using tree core samples and the first to observe the impacts past N-fixers have on current growth. The potential legacy effects N-fixers have on forest growth could further assist in understanding the wide variations previously observed in relation to neighborhood growth. Additionally, as it is known that N-fixers play a critical role in the land C sink, it is necessary to include past effects of N-fixation within biogeochemical models to accurately predict C sequestration as it relates to forest biomass.

Acknowledgements

I would like to thank the Grant-in-Aid of Research administered by Sigma Xi, The Scientific Research Society and the Columbia University MA grant for funding this project. I would like to thank my committee for their knowledge and guidance: Brendan Buckley, Duncan Menge, Matt Palmer, and Bill Schuster. I would also like to thank Evan Eskew, Michael Levin, Isobel Mifsud, Ryan Miller, Anika Staccone, Colleen Schmidt, and Emily Weisenberger for their input and assistance on various parts of my research. I also thank Alex Huddell and Wenying Liao for allowing me to incorporate data they collected in the summer of 2014 into my analyses. I would also like to thank Dan Helms and Dee Norris-Helms for very patiently editing this paper multiple times.

References

Adams, M.A., Turbull, T.L., Sprent, J.I., and Buchmann, N. 2016. Legumes are different: Leaf nitrogen, photosynthesis, and water use efficiency. Proc Natl Acad Sci USA. **113**: 4098 4103.

Batterman, S. A., Hedin, L. O., van Breugel, M., Ransijn, J., Craven, D. J., and Hall, J. S. 2013. Key role of symbiotic dinitrogen fixation in tropical forest secondary succession. Nature. **502**(7470): 224–227. doi: 10.1038/nature12525

Beghin, R., Cherubini, P., Battipaglia, G., Siegwolf, R., Saurer, M., and Bovio, G. 2011. Tree ring growth and stable isotopes (13 C and 15 N) detect effects of wildfires on tree physiological processes in *Pinus sylvestris* L. Trees. **25**: 627-636.

Boddey, R. M., M. B. Peoples, B. Palmer, and P. J. Dart. 2000. Use of the 15N natural abundance technique to quantify biological nitrogen fixation by woody perennials. Nutrient Cycling in Agroecosystems. **57**: 235–270.

Boring, L. R., and Swank, W. T. 1984. The role of black locust (*Robinia pseudoacacia*) in forest succession. The Journal of Ecology. 749-766

Binkley, D., Sollins, P., Bell, R., Sachs, D., and Myrold, D. 1992. Biogeochemistry of adjacent conifer and alder-conifer stands. Ecology. **73**(6): 2022-2033. doi: 10.2307/1941452

Binkley, D., K. Cromack Jr, and D. D. Baker. 1994. Nitrogen fixation by red alder: biology, rates, and controls. The biology and management of red alder. Oregon State University Press, Corvallis. 57–72.

Canham, C., LePage, P., Coates, K. 2004. A neighborhood analysis of canopy tree competition: Effects of shading versus crowding. Canadian Journal of Forest Research. **34**(4): 778-787.

Chapin, F. S., Conway, A. J., Johnstone, J. F., Hollingsworth, T. N., and Hollingsworth, J. 2016. Absence of net long-term successional facilitation by alder in a boreal Alaska floodplain. Ecology. **97**(11): 2986–2997. doi: 10.1002/ecy.1529

Chazdon, R.L., Letcher, S.G., Van Breugel, M., Martínez-Ramos, M., Bongers, F., and Finegan, B. 2007. Rates of change in tree communities of secondary Neotropical forests following major disturbances. Philosophical Transactions of the Royal Society of London B: Biological Sciences **362**: 273-289.

Danso, S. K. A., Zapata, F., Awonkaike, K. O. 1995. Measurement of biological N_2 fixation in field-grown *Robinia pseudoacacia* L. Soil Biology and Biochemsitry. **27**(4-5): 415-419.

Doughton, J. A., I. Vallis, and P. G. Saffigna. 1992. An indirect method for estimating 15 N isotope fractionation during nitrogen fixation by a legume under field conditions. Plant

and Soil. **144**: 23–29.

Feldpausch, T.R., Prates-Clark, C. da C., Fernandes, E.C.M., and Riha, S.J. 2007. Secondary forest growth deviation from chronosequence predictions in central Amazonia. Global Change Biology. **13**: 967-979.

Forrester, D. I., Bauhus, J., Cowie, A. L., and Vanclay, J. K. 2006. Mixed-species plantations of Eucalyptus with nitrogen-fixing trees: A review. Forest Ecology and Management, **233**(2–3): 211–230. doi: 10.1016/j.foreco.2006.05.012

Fyllas, N. M. et al. 2009. Basin-wide variations in foliar properties of Amazonian forest: Phylogeny, soils and climate. Biogeosciences. **6:** 2677-2708.

Gei, M., Rozendaal, D. M. A., Poorter, L., Bongers, F., Sprent, J. I., Garner, M. D., et al. 2018. Legume abundance along successional and rainfall gradients in Neotropical forests. Nature Ecology and Evolution. **2**(7): 1104–1111. doi: 10.1038/s41559-018-0559-6

Gerhart, L.M. and McLauchlan, K.K. 2014. Reconstructing terrestrial nutrient cycling using stable nitrogen isotopes in wood. Biogeochemistry. **120**(1-3): 1-21. doi: 10.1007/s10533 014-9988-8

Hietz, P., Turner, B.L., Wanek, W., Richter, A., Nock, C.A., and Wright, S.J. 2011. Long-term change in the nitrogen cycle of tropical forests. Science. **334**: 664-666.

Holmes, R. L. 1997. The Dendrochronology Program Library, p. 40-71. In: H. D. Grission-Mayer, R. L. Holmes and H. C. Fritts (eds.), The International Tree-Ring Data Bank Program Library Version 2.1 User's Manual. Laboratory of Tree-Ring Research, The University of Arizona, Tucson, AZ.

Hoogmoed, M., Cunningham, S. C., Baker, P., Beringer, J., and Cavagnaro, T. R. 2014. N-fixing trees in restoration plantings: Effects on nitrogen supply and soil microbial communities. Soil Biology and Biochemistry. **77**: 203–212. doi: 10.1016/j.soilbio.2014.06.008

Houlton, B. Z., Wang, Y., Vitousek, P. M., and Field, C. B. 2008. A unifying framework for dinitrogen fixation in the terrestrial biosphere. Nature. **454**: 327-330.

Kohl, D. H. and G. Shearer. 1980. Isotopic fractionation associated with symbiotic N_2 fixation and uptake of NO_3^- by plants. Plant Physiology. **66**: 51-56.

Lai, H.R., Hall, J.S., Batterman, S.A., Turner, B.L., and van Breugel, M. 2018. Nitrogen fixer abundance has no effect on biomass recovery during tropical secondary forest succession. Journal of Ecology. **106**(4): 1415-1427. doi: 10.1111/1365-2745.12979.

Liao, W., & Menge, D. N. L. 2016. Demography of symbiotic nitrogen-fixing trees explains their rarity and successional decline in temperate forests in the United States. PLoS ONE,

11(10): 1–13. doi: 10.1371/journal.pone.0164522

Marron, N., Gana, C., Gerant, D., Maillard, P., Priault, P., and Epron, D. 2018. Estimating symbiotic N_2 fixation in *Robinia pseudoacacia.* Journal of Plant Nutrition and Soil Science. **181**(2).

Mantovani, D., M. Veste, K. Boldt-Burisch, S. Fritsch, L. A. Koning, and D. Freese. 2015. Carbon allocation, nodulation, and biological nitrogen fixation of black locust (*Robinia pseudoacacia* L.) under soil water limitation. Annals of Forest Research. **58:** 259.

McLauchlan, K., Ferguson, C., Wilson, I., Ocheltree, Troy W., and Craine, Joseph M. 2010. Thirteen decades of foliar isotopes indicate declining nitrogen availability in central North American grasslands. New Phytologist. **187**(4): 1135-1145.

Meerts, P. 2002. Mineral nutrient concentrations in sapwood and heartwood: a literature review. Annals of Forest Science. **59**: 713-722.

Menge, D.N.L., and R. L. Chazdon. 2016. Higher survival drives the success of nitrogen-fixing trees through succession in Costa Rican rainforests. New Phytologist. Wiley Online Library. **209**: 965-977. doi: 10.1111/nph.13734

Menge, D. N. L., and L. O. Hedin. 2009. Nitrogen fixation in different biogeochemical niches along a 120, 000 year-chronosequence in New Zealand. Ecology. **90***:* 2190-2201

Menge, D. N. L., J. L. DeNoyer, and J. W. Lichstein. 2010. Phylogenetic constraints do not explain the rarity of nitrogen-fixing trees in late-successional temperate forests. PLoS One. **5**:e12056.

Menge, D. N. L., A. A. Wolf, and J. L. Funk. 2015. Diversity of nitrogen fixation strategies in Mediterranean legumes. Nature plants. **1**.

Merrill, W., and Cowling, E.B. 1966. Role of nitrogen in wood deterioration: amounts and distribution of nitrogen in tree stems. Canadian Journal of Botany. **44**: 1555-1580.

Minchin, F.R. and Witty, J.F. 2005. Respiratory/Carbon costs of symbiotic nitrogen fixation in legumes. *In* Plant Respiration: From Cell to Ecosystem, edited by Hans Lambers and Miquel Ribas-Carbo: 195-205. Advances in Photosynthesis and Respiration. Dordrecht: Springer Netherlands. doi: 10.1007/1-4020-3589-6_11

Minucci, J.M. 2017. Fixing nitrogen in a changing climate. uga.

Nasto, M.K., et al. 2014. Interactions among nitrogen fixation and soil phosphorous acquisition strategies in lowland tropical rain forests. Ecology Letters. **17**: 1282-1289.

Pearson, H. L. and P. M. Vitousek. 2002. Soil phosphorus fraction and symbiotic nitrogen fixation across a substrate-age gradient in Hawaii. Ecosystems. **5**: 587-596

Pellegrini, A. F. A., Staver, A. C., Hedin, L. O., Charles-Dominique, T., & Tourgee, A. 2016. Aridity, not fire, favors nitrogen-fixing plants across tropical savanna and forest biomes. Ecology. **97**(9): 2177–2183. doi: 10.1002/ecy.1504

Perakis, S. S., and Pett-Ridge, J. C. 2019. Nitrogen-fixing red alder trees tap rock-derived nutrients. PNAS. **116**(11): 5009-5014.

Phillips, D. L., and Gregg, J. W. 2001. Uncertainty in source partitioning using stable isotopes. Oecologia. **127**: 171-179. doi: 10.1007/s004420000578

Ruess, R. W., McFarland, J. M., Trummer, L. M., and Rohrs-Richey, J. K. 2009. Disease mediated declines in N-fixation inputs by *Alnus tenuifolia* to early-successional floodplains in interior and south-central Alaska. **12**: 489-502. doi: 10.1007/s10021-009 9237-5

Saurer, M., Cherubini, P. Ammann, M., De Cinti, B., and Siegwolf, R. 2004. First detection of nitrogen from NO_x in tree rings: A $^{15}N/^{14}N$ study near a motorway. Atmospheric Environment. **38**: 2779-2787.

Schulze, J., et al. 1999. Carbon costs associated with N2 fixation in Vicia Faba L. and Pisum Sativum L. over a 14 day period. Plant Biology. **1**(6): 625-631. Doi: 10.1055/s-2007 978565

Schuster, W. 2019. Personal communication.

Schuster, W., and Hutnik, R. 1987. Community development on 35-year-old planted minespoil banks in Pennsylvania. Reclamation and Revegetation Research. **6**: 109–120.

Schuster, W. S. F., K. L. Griffin, H. Roth, M. H. Turnbull, D. Whitehead, and D. T. Tissue. 2008. Changes in composition, structure and aboveground biomass over seventy-six years (1930-2006) in the Black Rock Forest, Hudson Highlands, southeastern New York State. Tree physiology. **28***:* 537–549.

Shearer, G., and D. H. Kohl. 1986. N2-fixation in field settings: estimations based on natural 15N abundance. Functional Plant Biology. **13***:* 699–756.

Sheppard, P. R., and T. L. Thompson. 2000. Effect of extraction pretreatment on radial Variation of nitrogen concentration in tree rings. Journal of Environmental Quality. **29***:* 2037–2042.

Shi, Z., Yang, Y., Zhou, X., Weng, E., Finzi, A. C., & Luo, Y. 2016. Inverse analysis of coupled carbon-nitrogen cycles against multiple datasets at ambient and elevated CO2. Journal of Plant Ecology. **9**(3*):* 285–295. doi: 10.1093/jpe/rtv059

Siddique, I., Engel, V. L., Parrotta, J. A., Lamb, D., Nardoto, G. B., Ometto, J. P. H. B., et

al. 2008. Dominance of legume trees alters nutrient relations in mixed species forest restoration plantings within seven years. Biogeochemistry. **88**(1): 89–101. doi: 10.1007/s10533-008-9196-5

Soper, F.M., Boutton, T.W., and Sparks, J.P. 2015. Investigating patterns of symbiotic nitrogen fixation during vegetation change from grassland to woodland using fine scale $\delta^{15}N$ abundance. Functional Plant Biology. **13**: 699-756.

Staccone, A., Kou-Giesbrecht, S., Taylor, B., and Menge, D. In Review. Nitrogen-fixing trees do not facilitate forest growth across the coterminous United States.

Staccone, A., Liao, W., Perakis, S., Compton, J., Clark, C.M., and Menge, D.N.L. 2020. A spatially explicit, empirical estimate of tree-based biological nitrogen fixation in forests of the United States. Global Biogeochemical Cycles. doi: 10.1029/2019GB006241

Stokes, M.A. 1996. An introduction to tree-ring dating. University of Arizona Press.

Sullivan, B. W., Smith, W. K., Townsend, A. R., Nasto, M. K., Reed, S. C., Chazdon, R. L., and Cleveland, C. C. 2014. Spatially robust estimates of biological nitrogen (N) fixation imply substantial human alteration of the tropical N cycle. Proceedings of the National Academy of Sciences. 201320646

Taylor, B. N., Chazdon, R. L., Bachelot, B., & Menge, D. N. L. 2017. Nitrogen-fixing trees inhibit growth of regenerating Costa Rican rainforests. Proceedings of the National Academy of Sciences. **114**(33): 8817–8822. doi: 10.1073/pnas.1707094114

Taylor, B. N. and Menge, D. N. L. 2018. Light regulates tropical symbiotic nitrogen fixation more strongly than soil nitrogen. Nature Plants. **4**(9): 655-661.

Team, R. C. 2018. R: R: A language and environment for statistical computing. R Foundation for Statistical Computing, Vienna, Austria. URL https://www.R-project.org/.

Townsend, A.R., Cleveland, C.C., Asner, G.P., and Bustamante, M.M.C. 2007. Controls over foliar N:P ratios in tropical rain forests. Ecology. **88**: 107-118

Uliassi, D. D., and R. W. Ruess. 2002. Limitations to symbiotic nitrogen fixation in primary succession on the Tanana River floodplain. Ecology. **83***:* 88-103.

Unkovich, M.J., and Pate, J.S. 2000. An appraisal of recent field measurements of symbiotic N_2 fixation by annual legumes. Field Crops Research. **65**(2-3): 211-228. doi: 10.1016/S0378-4290(99)00088-X

van Kessel, Chris, Farrell, Richard E., Roskoski, Joann P., Keane, Kevin M. 1994. Recycling of the naturally-occurring ^{15}N in an established stand of *Leucaena leucocephala*. Soil Biology and Biochemistry. **26**(6): 757-762. doi: 10.1016/0038-0717(94)90269-0

Viereck, L. A., Dyrness, C. T., and Foote, M. J. 1993. An overview of the vegetation and soils of the floodplain ecosystems of the Tanana River, interior Alaska. Canadian Journal of Forest Research. **23**: 889-898.

Wedderburn, M.E. and Carter, J. 1999. Litter decomposition by four functional tree types for use in silvopastoral systems. Soil Biology and Biochemistry. **31**(3): 455-461.

Winbourne, J.B., Feng, A., Reynolds, L., Piotto, D., Hastings, M.G., and Porder, S. 2018. Nitrogen cycling during secondary succession in Atlantic Forest of Bahia, Brazil. Scientific reports. **8**: 1377.

Wurzburger, N., and Miniat, C.F. 2014. Drought enhances symbiotic dinitrogen fixation and competitive ability of a temperate forest tree. Oecologia. **174**: 1117-1126.

Tables

Table 1. The predicted changes in growth rate of neighboring trees when going from no crowding from N-fixers to only crowding from N-fixers for each model calculated from the corresponding coefficient values.

Model Equation	Proportion of crowding from N-fixers coefficient value (SE)	N-Fixer effect on Relative Growth Rate (-SE, +SE)
Eq. 9	0.167 (.05)	18.2% (12.5%, 24.2%)
Eq. 10	0.168 (.05)	18.3% (12.5%, 24.2%)
Eq. $11_{\text{N-fixer}}$	-0.05 (.176)	-5% (-20.3%, 13.5%)
Eq. $11_{\text{Non-fixer}}$	0.13 (.064)	13.9% (6.8%, 21.4%)
Eq. $12_{\text{N-fixer}}$	-0.064 (.178)	-6.2% (-21.5%, 12%)
Eq. $12_{\text{Non-fixer}}$	0.135 (.064)	14.5% (7%, 22%)
Eq. $13_{\text{1-year lag}}$	0.186(.048)	20.4% (14.8%, 26.3%)

Figures

Figure 1. Nitrogen isotope ratios ($\delta^{15}N$) in tree cores of *Robinia pseudoacacia* and *Prunus serotina* trees and the corresponding estimated percent nitrogen derived from fixation ($\%N_{dfa}$) in *Robinia*. Two sites are shown: (a, c) the Upper Reservoir site and (b, d) the Stone House site. (a, b) $\delta^{15}N$ values were measured from 5 year segments of tree cores. Blue points are data from *Prunus* trees. Red, orange and yellow points are data from *Robinia* trees. Each color corresponds to an individual tree. The black solid and dotted lines represent the mean ± standard deviation of the end member we used for the pure nitrogen fixation signal. The $\delta^{15}N$ values were used to calculate the $\%N_{dfa}$ values and their 95% confidence intervals in (c, d). (c, d) Each point represents the mean $\%N_{dfa}$ value for a given 5-year time segment. Horizontal values were jittered for visibility. Each color is an individual *Robinia* tree, corresponding to (a, b). The black error bars represent the upper and lower 95% confidence intervals of the mean $\%N_{dfa}$ value. The red, orange, and yellow lines are the mean $\%N_{dfa}$ values for the individual trees based on the best fit model. Note the different vertical scales in (c) and (d).

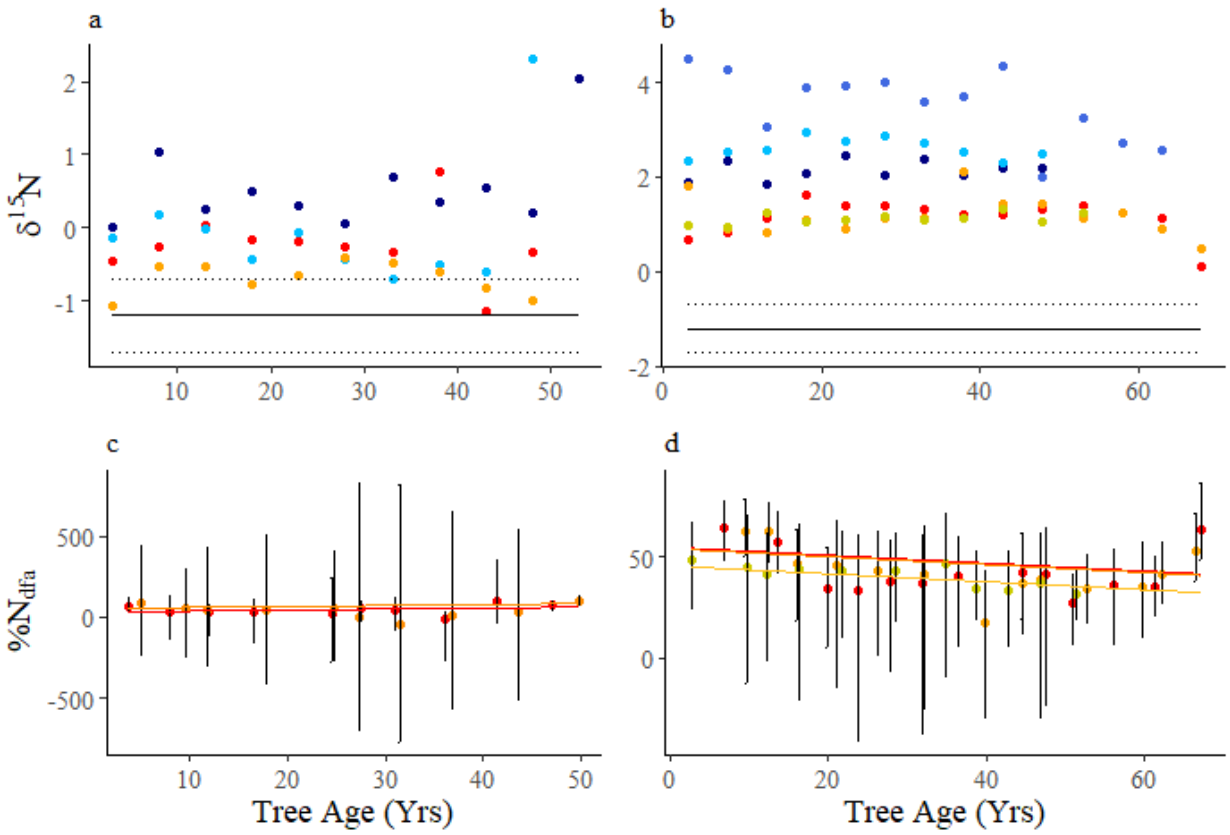

a
b
c
d
δ15N
%Ndfa
Tree Age (Yrs)
Tree Age (Yrs)

Figure 2. Effect of crowding from N-fixers on relative growth rate (yr^{-1}) for all trees present at both the Stone House and Upper Reservoir sites. Blue circles are the median growth rate values of non-fixing trees of various species and red triangles are the median growth rate values of *Robinia pseudoacacia* trees. Vertical lines passing through all points represent the range of values for an individual tree's annual relative growth rate. (a) The best fit model, with the lowest AIC, had a single interaction (between the control drivers, DBH and NCI) and no quadratic term (Eq. 9). The black line refers to the best fit for all trees together. The blue and red lines are the best fits for non-fixers and N-fixers, respectively. The black, red, and blue lines are all plotted at the mean value of NCI and DBH. (b) The best fit models as shown in (a) plotted against the datapoints for an average tree with average crowding. This eliminates any noise due to tree size and total crowding. These plots show the overall effect N-fixers have on neighboring trees, non-fixers and N-fixers alike, independent of tree size and total tree crowding.

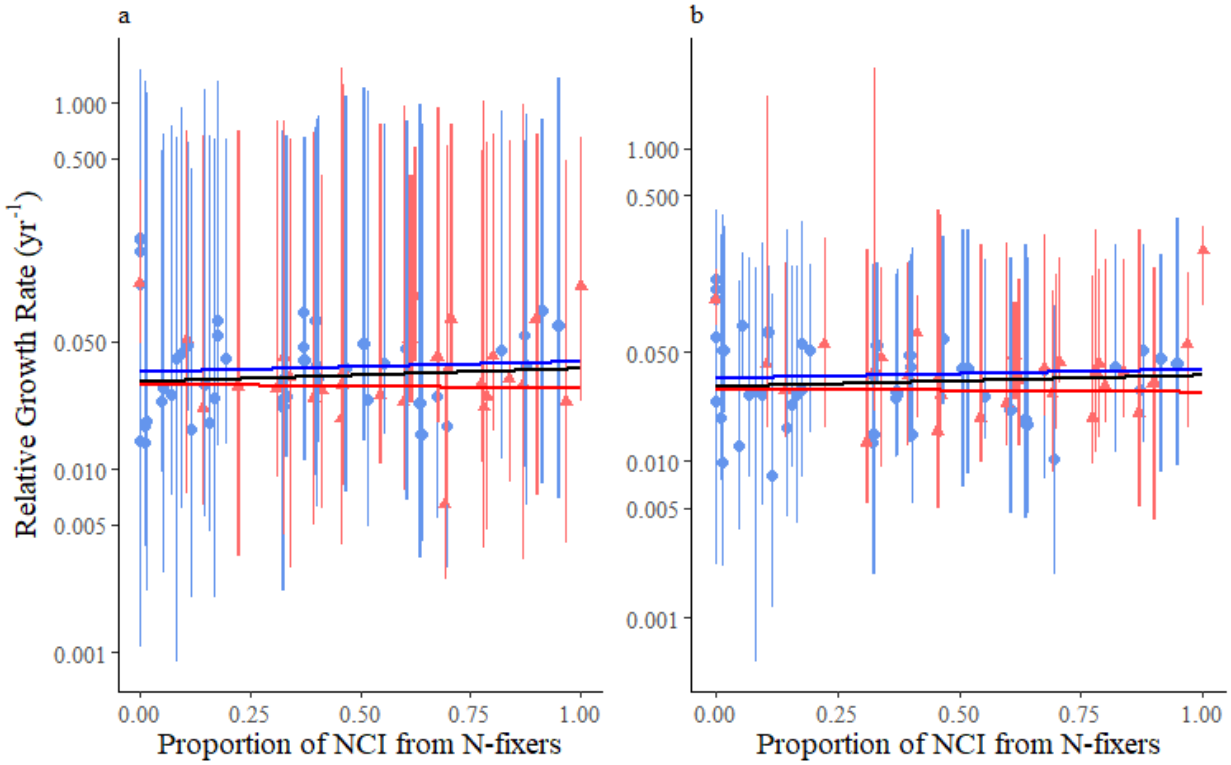
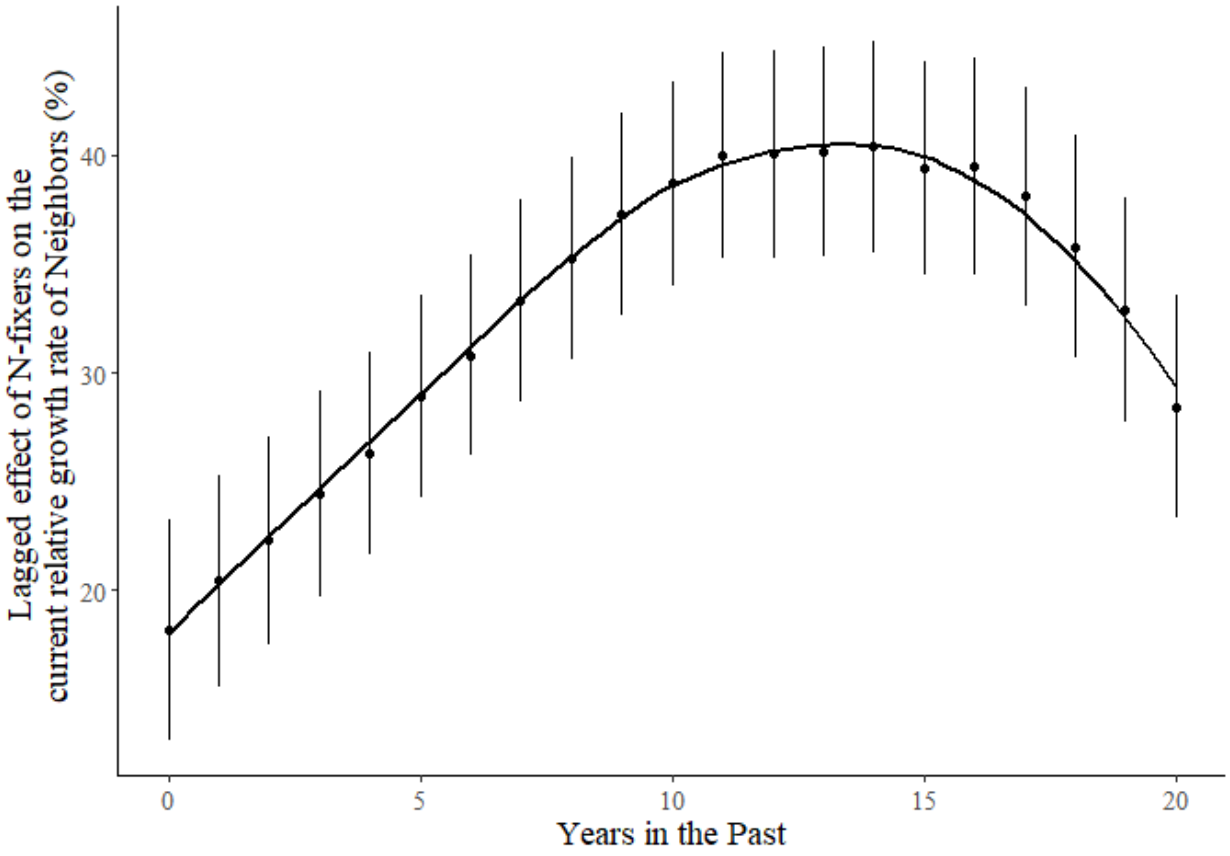


Figure 3. Effect of past crowding by *Robinia pseudoacacia* on the relative growth rate of neighboring trees. Each black dot is calculated from a coefficient value related to the response of RGR to the proportion of NCI from N-fixers at different times in the past, from 1 year to 20 years. Specifically, the plotted coefficient values are N-fixer effects, as in Staccone et al. (in review), which describe the percent change in RGR in a scenario where all neighbors (at a given time in the past) were N fixers vs. a scenario where all neighbors (at the same time) were all non-fixers. The black curve is the loess fit for the data points. The black error bars are the standard errors predicted from the model.



Supplementary Information

Master's Thesis

Lex Helms

SI. Text 1. We ran various models using relative growth rate (log-transformed to ensure normality) as a function of the total NCI around an individual, the DBH of the individual, and the proportion of NCI from *Robinia*, as follows:

$$\ln(RGR_i) = \alpha + \beta_1 NCI_{prop,\,i} + \beta_2 DBH_i + \beta_3 NCI_i + \varepsilon \quad \text{SI Eq. 1}$$

$$\ln(RGR_i) = \alpha + \beta_1 NCI_{prop,\,i} + \beta_2 DBH_i + \beta_3 NCI_i + \beta_4 NCI_i^2 + \varepsilon \quad \text{SI Eq. 2}$$

$$\ln(RGR_i) = \alpha + \beta_1 NCI_{prop,\,i} + \beta_2 DBH_i + \beta_3 NCI_i + \beta_4 NCI_i x DBH_i + \varepsilon \quad \text{SI Eq. 3}$$

$$\ln(RGR_i) = \alpha + \beta_1 NCI_{prop,\,i} + \beta_2 DBH_i + \beta_3 NCI_i + \beta_4 NCI_i^2 + \beta_5 NCI_i x DBH_i + \varepsilon \quad \text{SI Eq. 4}$$

$$\ln(RGR_i) = \alpha + \beta_1 NCI_{prop,\,i} + \beta_2 DBH_i + \beta_3 NCI_i + \beta_4 NCI_{prop,\,i}\, x DBH_i + \varepsilon \quad \text{SI Eq. 5}$$

We also ran versions of the model considering N-fixers and non-fixers separately, as a binary term:

$$\ln(RGR_i) = \alpha + \beta_1 NCI_{prop,\,i} + \beta_2 DBH_i + \beta_3 NCI_i + \beta_4 \text{N-fixer} + \beta_5 NCI_{prop,\,i}\, x \text{N-fixer} + \varepsilon \quad \text{SI Eq. 6}$$

$$\ln(RGR_i) = \alpha + \beta_1 NCI_{prop,\,i} + \beta_2 DBH_i + \beta_3 NCI_i + \beta_4 NCI_i^2 + \beta_5 \text{N-fixer} + \beta_6 NCI_{prop,\,i}\, x \text{N-fixer} + \varepsilon \quad \text{SI Eq. 7}$$

$$\ln(RGR_i) = \alpha + \beta_1 NCI_{prop,\,i} + \beta_2 DBH_i + \beta_3 NCI_i + \beta_4 \text{N-fixer} + \beta_5 NCI_{prop,\,i}\, x \text{N-fixer} + \beta_5 NCI_i x DBH_i + \varepsilon \quad \text{SI Eq. 8}$$

$$\ln(RGR_i) = \alpha + \beta_1 NCI_{prop,\,i} + \beta_2 DBH_i + \beta_3 NCI_i + \beta_4 NCI_i^2 + \beta_5 \text{N-fixer} + \beta_6 NCI_{prop,\,i}\, x \text{N-fixer} + \beta_7 NCI_i x DBH_i + \varepsilon \quad \text{SI Eq. 9}$$

$$\ln(RGR_i) = \alpha + \beta_1 NCI_{prop,\,i} + \beta_2 DBH_i + \beta_3 NCI_i + \beta_4 \text{N-fixer} + \beta_5 NCI_{prop,\,i}\, x \text{N-fixer} + \beta_7 NCI_{prop,\,i}\, x DBH_i + \varepsilon \quad \text{SI Eq. 10}$$

To address the possibility of lag effects between the presence of *Robinia* and neighbor growth rate, we ran models using relative growth rate as a function of past crowding from N-fixers from 1-20 years ago:

$$\ln(RGR_i) = \alpha + \beta_1 NCI_{prop,\, i,\, lagged} + \beta_2 DBH_i + \beta_3 NCI_i + \beta_4 DBH_i \times NCI_i + \varepsilon \qquad \text{SI Eq. 11}$$

We also ran models using relative growth rate as a function of past crowing from N-fixers and total past crowding from 1-20 years ago:

$$\ln(RGR_i) = \alpha + \beta_1 NCI_{prop,\, i,\, lagged} + \beta_2 DBH_i + \beta_3 NCI_{i,\, lagged} + \beta_4 DBH_i \times NCI_{i,\, lagged} + \varepsilon \qquad \text{SI Eq. 12}$$

For all models, α is the overall intercept, βs are the regression coefficients, and ε is the normally distributed error term. All of the best models were linear with the driver variable of interest, the proportion of NCI from *Robinia.*

SI Table 1. Estimated $\%N_{dfa}$ intercept and slope values for the relationship between age and $\%N_{dfa}$ in *Robinia pseudoacacia* from the best fit model. $Nfixer_1$ and $Nfixer_2$ are the individual N-fixing trees sampled on that site. SH and UR are Stone House and Upper Reservoir sites.

Parameter (units)	Coefficient value (SE)	z value	Pr(z)
$Intercept_{Nfixer1,UR}$ (%)	32.3 (13.1)	2.47	0.0134
$Intercept_{Nfixer2,UR}$ (%)	54.4 (15.0)	3.62	0.0003
$Slope_{UR}$ (% yr^{-1})	0.6 (0.4)	1.73	0.8383
$Intercept_{Nfixer1,SH}$ (%)	55.0 (3.96)	13.9	< 2e-16
$Intercept_{Nfixer2,SH}$ (%)	54.3 (4.02)	13.5	< 2e-16
$Intercept_{Nfixer3,SH}$ (%)	45.8 (4.02)	11.4	< 2e-16
$Slope_{SH}$ (% yr^{-1})	-0.2 (0.07)	-2.71	0.0066

SI Table 2. Model results from the best fit model for the effect of the proportion of crowding from N-fixer *Robinia pseudoacacia* (NCI_{prop}) on the log-transformed relative growth rate of neighboring trees. In addition to the proportion of crowding from *Robinia*, this model included total crowding (NCI), tree size (DBH), and the interaction between DBH and NCI.

Parameter (units)	Coefficient value (SE)	t value	Pr(>|t|)
Intercept (m yr^{-1})	-2.09 (0.04)	-57.8	< 2e-16
NCI_{prop}	0.17 (0.05)	3.37	0.0008
NCI_{total}	-24.7 (1.20)	-12.4	< 2e-16
DBH (m yr^{-1})	-21.4 (0.47)	-45.4	< 2e-16
NCI_{total}: DBH	202.7 (15.8)	12.8	< 2e-16

SI Table 3. Model results from the second best fit model for the effect of the proportion of crowding from N-fixer *Robinia pseudoacacia* (NCI_{prop}) on the log-transformed relative growth rate of neighboring trees. This model included all drivers as the best fit model as well as a quadratic term (NCI^2).

Parameter (units)	Coefficient value (SE)	T value	Pr(>|t|)
Intercept (m yr^{-1})	-2.09 (0.04)	-57.4	< 2e-16
NCI_{prop}	0.17 (0.05)	3.38	0.0007
NCI_{total}	-25.2 (2.43)	-10.4	< 2e-16
DBH (m yr^{-1})	-21.3 (0.54)	-39.8	< 2e-16
NCI_{total}^2	6.15 (15.9)	0.39	0.6980
NCI_{total}: DBH	201.4 (16.2)	12.4	< 2e-16

SI Table 4. Model results from the best fit model that separated out N-fixer vs. non-fixer growth. This model is similar to the one in Table 2, except that it also examines the effects of whether the focal tree is an N-fixer or not on both the intercept and the effect of the proportion of crowding from *Robinia*.

Parameter (units)	Coefficient value (SE)	T value	Pr(>|t|)
Intercept (m yr^{-1})	-2.12 (0.04)	-55.6	< 2e-16
NCI_{prop}	0.13 (0.06)	2.02	0.0427
NCI_{total}	-25.2 (2.00)	-12.6	< 2e-16
DBH (m yr^{-1})	-21.4 (0.47)	-45.6	< 2e-16
N-Fixer (m yr^{-1})	0.24 (0.06)	3.85	0.0001
NCI_{prop}:N-Fixer	-0.18 (0.11)	-1.60	0.1091
NCI:DBH	199.9 (15.8)	12.64	<2e-16

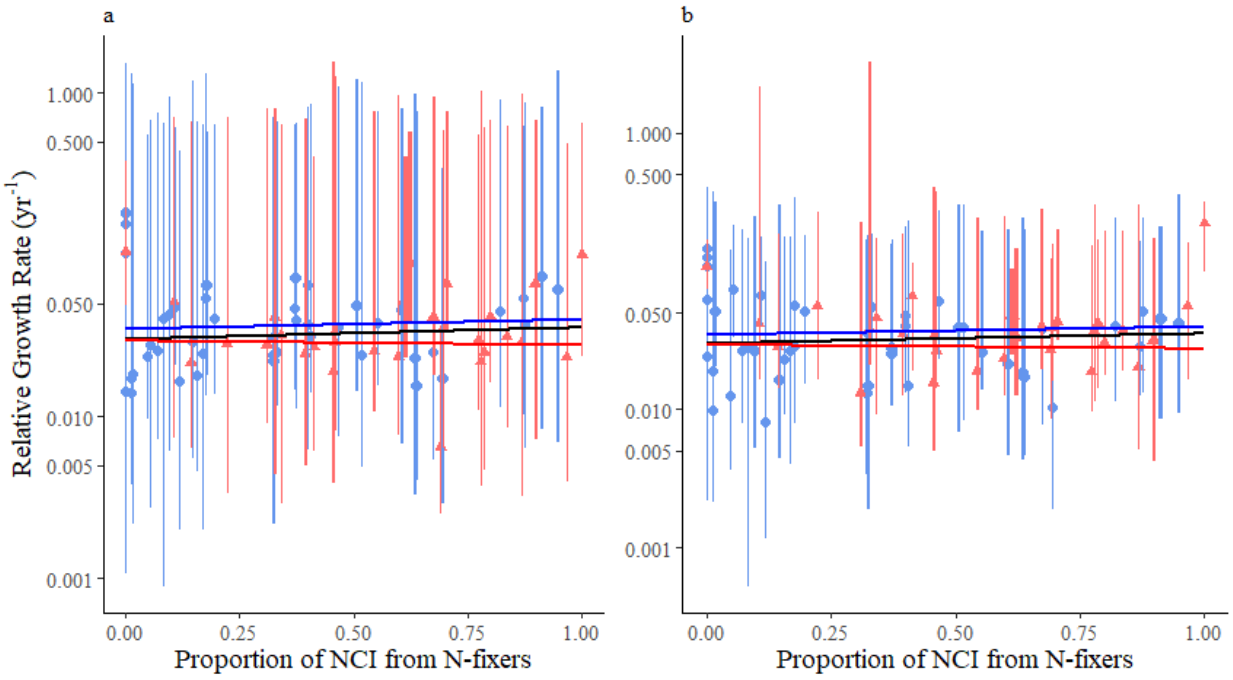
SI Table 5. Model results from the second best fit model that separated out N-fixer vs. non-fixer growth. This model is similar to the one in Table 4, except that it also includes a quadratic term (NCI^2).

Parameter (units)	Coefficient value (SE)	T value	Pr(>|t|)
Intercept (m yr^{-1})	-2.13 (0.04)	-54.9	< 2e-16
NCI_{prop}	0.14 (0.06)	2.11	0.0354
NCI_{total}	-26.8 (2.45)	-10.9	< 2e-16
DBH (m yr^{-1})	-21.1 (0.54)	-39.4	< 2e-16
NCI^2	18.9 (16.1)	1.18	0.2385
N-Fixer (m yr^{-1})	0.26 (0.06)	3.99	6.48e-05
NCI_{prop}:N-Fixer	-0.199 (0.11)	-1.76	0.0791
NCI:DBH	195.7 (16.2)	12.1	<2e-16

SI Table 6. Model results from one of the time-lag models. This model is similar to the one in Table 2, except that the effects of total crowding (NCI) and the proportion of crowding from N fixers (NCI_{prop}) are lagged by one year.

Parameter (units)	Coefficient value (SE)	T value	Pr(>|t|)
Intercept (m yr^{-1})	-2.26 (0.04)	-64.3	< 2e-16
$NCI_{prop,\ 1\ yr}$	0.19 (0.05)	4.10	4.15e-05
$NCI_{total,\ 1\ yr}$	-23.2 (1.96)	-11.9	< 2e-16
DBH (m yr^{-1})	-19.1 (0.45)	-41.9	< 2e-16
$NCI_{total,\ 1\ yr}$: DBH	173.7 (15.4)	11.2	<2e-16

SI Figure 1. Effect of crowding from N-fixers on relative growth rate (m yr^{-1}) for all trees present at both the Stone House and Upper Reservoir sites. Blue circles are the median growth rate values of non-fixing trees of various species and red triangles are the median growth rate values of *Robinia pseudoacacia* trees. Vertical lines passing through all points represent the range of values for an individual tree's annual relative growth rate. (a) The second best fit model had a single interaction (between the control drivers, DBH and NCI) and a quadratic term (Eq. 10). The black line refers to the best fit for all trees together. The blue and red lines are the best fits for non-fixers and N-fixers, respectively from the second best model (Eq. 12). The black, red, and blue lines are all plotted at the mean value of NCI and DBH. (b) The best fit models as shown in (a) plotted against the datapoints for an average tree with average crowding. This eliminates any noise due to tree size and total crowding. These plots show the overall effect N-fixers have on neighboring trees, non-fixers and N-fixers alike, independent of tree size and total tree crowding.



SI Figure 2. Effect of past crowding by *Robinia pseudoacacia* and past total crowding on the relative growth rate of neighboring trees. Each black dot is calculated from a coefficient value related to the response of RGR to the proportion of NCI from N-fixers at different times in the past, from 1 year to 20 years. The plotted coefficient values are N-fixer effects, as in Staccone et al. (in review), which describe the percent change in RGR in a scenario where all neighbors (at a given time in the past) were N fixers vs. a scenario where all neighbors (at the same time) were all non-fixers. The black curve is the loess fit for the data points. The black error bars are the standard errors predicted from the model.

